

**Tectonic Development of Wadi Miar, Sinai, Egypt: Implications of Low-Temperature Thermochronology Techniques****Sherif Mansour\***

Geology Department, Faculty of Science, Port Said University, Port Said 42522, Egypt

**\*Corresponding author: [sherif@sci.psu.edu.eg](mailto:sherif@sci.psu.edu.eg)**

---

**ABSTRACT**

The basement rocks of Wadi Mi'ar, cropping out along the eastern flank of the Suez Rift, constitute part of the NE segment of the Neoproterozoic Arabian-Nubian Shield. The whole region is finally reshaped by the Suez Rift initiation during the Oligocene-Miocene. Low-temperature thermochronology techniques are capable of providing new insights into the tectonic development of the Suez Rift by reconstructing the uplifting response of its flanks. Therefore, we provide here thermochronological data for seven collected samples from the basement rocks of the Suez Rift's eastern flank at Wadi Mi'ar. Zircon fission-track technique yielded cooling ages of  $339 \pm 10$  Ma and  $334 \pm 9$  Ma. While the apatite fission-track dated samples yielded ages between  $26 \pm 5$  Ma and  $21 \pm 4$  Ma. These cooling ages and the time-temperature modelling revealed three possible cooling pulses that represent exhumation events which were initiated as a response to three tectonic events; (1) the Neoproterozoic post-accretion erosional event, (2) the Devonian-Carboniferous Hercynian tectonic event, and (3) the Oligocene-Miocene Suez Rift. Furthermore, the Suez Rift initiation was accompanied by more than 3 km of rift flanks uplift to exhume samples from depths equivalent to 110 °C (apatite fission-track partial annealing zone) in the studied region. While the northern portion of the flank is dominated by older thermochronologic ages and modest rift flanks elevations.

**Key Words:**

Arabian-Nubian Shield, Sinai fission-track, Egypt thermochronology, Fission-track, The Suez Rift.

---

**1- INTRODUCTION**

The Gulf of Suez as the northern extend of the Red Sea is a continental lithospheric rift system that developed partially, in the Red Sea, into a seafloor spreading stage. The rift processes can be studied indirectly through its flanks, which are formed from basement rocks of the Arabian Nubian Shield (ANS) (Fig. 1). The ANS was initially established between ca. 900–650 Ma as the northern part of the East African Orogeny (EAO; [1]–[3]). The Egyptian ANS (ENS) rocks in North Eastern Desert (NED) and South Sinai are equivalent, where the frequent occurrence of the post-tectonic (ca. 622-535 Ma; [4]) Younger Granitoids, dike suits, and volcano-sedimentary successions, and lesser existence of Older Granitoids and ophiolites [4]–[12]. The felsic to intermediate Dokhan Volcanics [13] is the main volcanic event in the NED (630-590 Ma; [14]).

After growth during the Ediacaran [4], the ENS was completely eroded by Cambrian time, marked by the development of a peneplain surface (e.g., [15]). Afterwards, a ca. 2.5 km thickness sedimentary succession of Lower Palaeozoic age started to accumulate (e.g., [16]). This regime was interrupted by the Devonian-Carboniferous Hercynian tectonic event, which affected the region through a sequence of uplifts and erosions (e.g., [17]). Then, a phase of thermo-tectonic stability dominated until the Cretaceous [18], when the Mid-Atlantic initiation affected the region by the development of the Syrian arc system (e.g., [19]–[21]). Shortly after, the Red Sea/Suez rifting processes started by the Oligocene-Miocene, developing grabens at the rift axis and elevated flanks. Reconstructing the thermo-tectonic history of the Suez rift and its Ediacaran ENS basement flanks. (Fig. 1) can be achieved by thermochronological analysis (e.g., [22]–[24]). Several thermochronological studies have taken place on the rift system flanks of the Red Sea, the Gulf of Aqaba, and the eastern Gulf of Suez (e.g., [16], [24]–[32]). Whilst, fewer attention was given to the western flank of the Suez Rift [11], [33]. This is responsible for information shortage which could illustrate issues related to the thermos-tectonic history of the region, the Gulf of Suez rift type, and the heterogeneity of its elevated flanks.

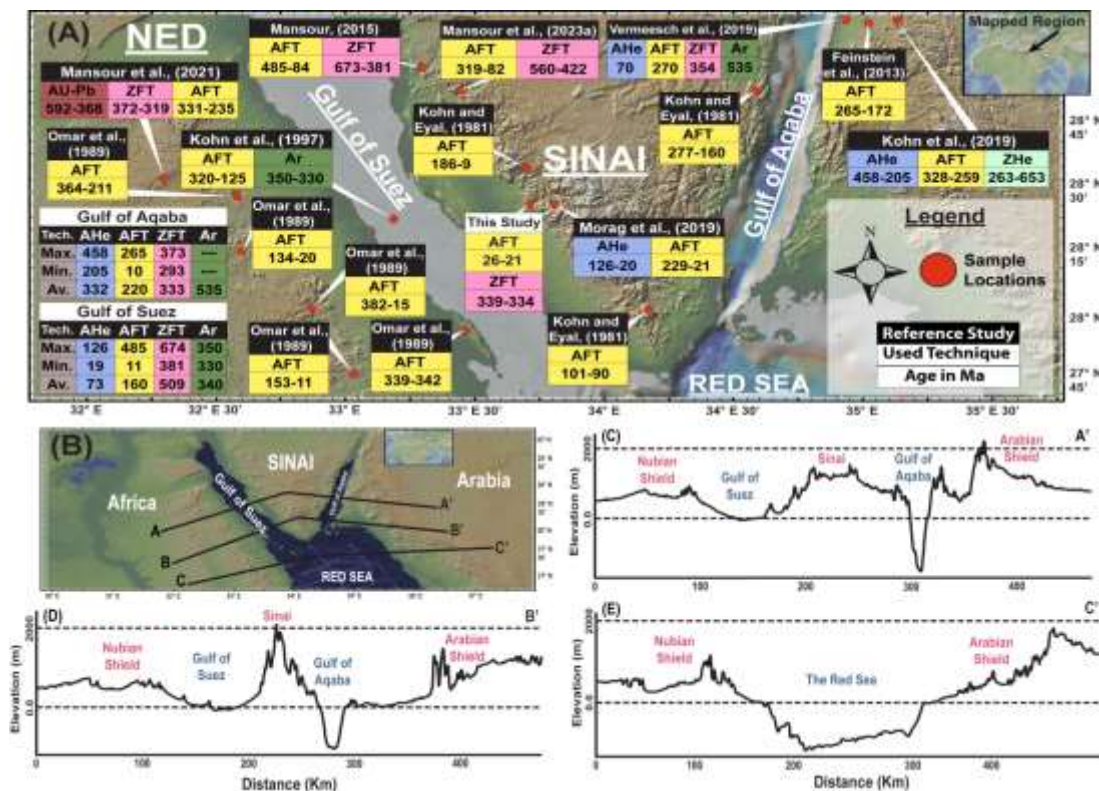


**Fig. (1): A.** Location map of the northern ANS locating the reported thermochronological data (modified after [34]). Where, Ar = Ar-Ar ages; ZFT= zircon fission-track ages, AFT= apatite fission-track ages, ZHe; zircon (U-Th)/He ages, and AHe; apatite (U-Th)/He ages.

**B.** Locations of the represented topographic cross sections.

To address these issues, we applied zircon fission-track (ZFT), apatite fission-track (AFT) thermochronology techniques, and time-temperature (t-T) modelling on seven samples from the Wadi Mi'ar area, at the eastern flank of the Suez Rift (Fig. 2).

## 2- GEOLOGIC SETTING

The Red Sea/Suez Rift system initiation was triggered by the Afar superplume activities by ca. 34 Ma [35]–[38], along with the Bitlis-Zagros subduction and the following convergence zone in modern

Anatolia [39]. The first (ca. 45 Ma) and second (31-29 Ma) voluminous volcanism in the Afar triple junction where focused along its vicinity at Kenya, Ethiopia, and Yemen [40]–[44]. Then, this activity migrated further northward by ca. 28 Ma, forming the Older Harrats along the Arabia's western margin [43]. Afterwards, volcanisms and dike swarms activated along the western margin of Arabia by 24-21 Ma, which is chemically comparable to the Afar plume [43]. These magmatic activities were accompanied by the main extensional event ( $24 \pm 2.2$  Ma) propagating northward through the Suez rift [25], [31], [45]–[47]. As a consequence, elevated flanks formed along the central and northern Red Sea [11], [24], [28], [30], [33], [48]. Then, a second flanks uplift phase (ca. 15 Ma) is recorded in central Arabia [48]. Shortly after, another volcanic activity was initiated (ca. 13 Ma) in western Arabia, forming the Younger Harrats [49].

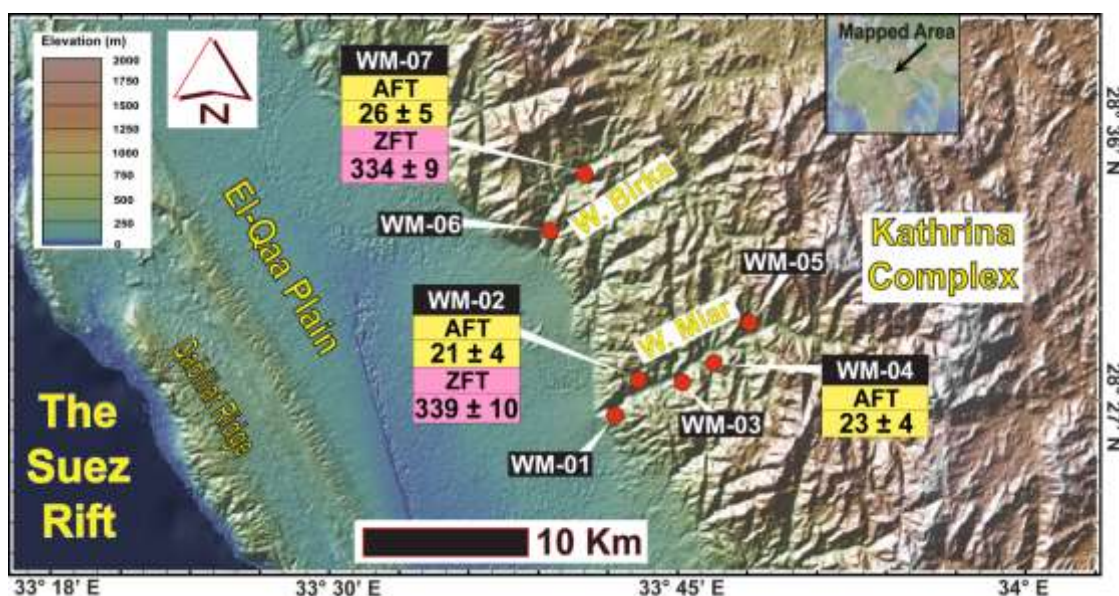


**Fig. (2):** Topographic and location map for the Wadi Mi'ar area showing localities of the analyzed samples, and ZFT and AFT ages.

The Red Sea rift system is flanked by the basement rocks of the ANS which is initially formed through oceanic plateaus, island arcs, and continental fragments accretion during the EAO between ca. 900 Ma and 650 Ma (e.g., [2], [4]). These basement rocks in NED are constructed mainly of (1) island arc metamorphic suite representing the EAO oldest activity that prolonged between ca. 820 Ma and 750 Ma (e.g., [4], [50]). (2) syn-orogeny alkaline and calc-alkaline granitoid suite characterizing the EAO compressional stage that extended from ca. 750 to 610 Ma. (e.g., [4], [51]). (3) post-orogeny alkaline and calc-alkaline granitoid, and dike swarm suites representing the EAO extensional phase that dominated from ca. 610 Ma and 535 Ma [4], [51], [52].

After the EAO, a post-accretion event of intense erosion (PAEE) entirely removed the ENS high topography before Cambrian time. This is documented by identifying fossils with Early Cambrian ages in near shore to fluvial sediments (e.g., [53], [54]). This sedimentation was sustained until the Devonian deposited a Lower Paleozoic sequence of more than 2.5 Km. During the boundary between the Devonian and the Carboniferous, the Variscan or the Hercynian tectonic activity was developed by the impact between Laurasia and Gondwana [55]. This collision initiated significant uplifts and erosions in the Lower Palaeozoic sequence of the NED and Sinai (e.g., [25], [56]–[58]). While, a complete succession is preserved in southern Jordan and northern Saudi Arabia (e.g., [59]). Throughout the boundary between the Jurassic and the Cretaceous, the Gondwana breakup initiated affecting northern Egypt by sinistral shearing, localized volcanic activities, and the Syrian Arc system [19]–[21], [60], [61]. Through the boundary between the Oligocene and the Miocene, the Red Sea/Suez Rift system initiated producing elevated rift flanks, normal faults, and restricted basic dykes.

There is a debate about the type of the northern Red Sea/Suez rift and the proposed existence of an additional thermal overprint. Furthermore, the cause of the topographic heterogeneity between the Suez Rift western flank and eastern flank, and between Africa and Arabia (Fig. 1B). One model for the Suez



Rift initiation suggests a mechanical rift type where the flanks exhumed by an isostatic rebound to rift axis development [31], [33]. A second model considers an additional southward thermal effect [32], [62]. A third proposed model recommends a major effect of the anticipated mini mantle plume of Cairo [24], [63], or the plume at the Arabian Red Sea margin.

### 3- METHODS AND TECHNIQUES

The fission-track low-temperature thermochronology technique is counting on the accumulation of the etchable radiation damage (tracks) of the spontaneous  $^{238}\text{U}$  fission in the crystal lattice [64]. Retention, reservation and annealing of these fission-related tracks are sensitive to temperature zones that differ according to the analyzed mineral [65], [66], which enables time-temperature (t-T) history reconstruction. The zircon mounts were etched in a eutectic melt of NaOH–KOH at  $220 \pm 5^\circ\text{C}$  [67] for 50–75 minutes. While, the apatite mounts were etched for 20 seconds in 5.5N HNO<sub>3</sub> at  $20 \pm 1^\circ\text{C}$  (e.g., [68]). Ages and error ranges were calculated using IsoplotR [69].

Thermal/tectonic history modelling was performed using the computer program HeFTy v1.9.1 [70]. The constraints guiding the Monte-Carlo algorithm were chosen as; initial constraints with Neoproterozoic age (at depth), near-surface between the Neoproterozoic and the Cambrian (the PAEE), ZFT ages (whenever measured), the AFT obtained ages, and the Suez Rift opening time. Models were run until producing a 100 good model, these are the produced t-T paths with  $\geq 50\%$  goodness of fit (GOF) between the model and the measured inputted data. Additionally, HeFTy calculates the best path with the highest GOF which is displayed in black, and the t-T path with weighted mean values of all models which is displayed in blue [71], [72].

To achieve the aims of this study, we have collected seven samples from Wadi Mi'ar which is located on the Suez Rift's eastern flank (Fig. 2). Among them 2 samples yielded enough zircons, 3 samples provided suitable apatites for fission-track analyses (Fig. 2), and 2 samples provided sufficient horizontal confined tracks for t-T modelling.

### 4- RESULTS AND DISCUSSION

From the seven analyzed samples, 2 samples provided appropriate zircon grains for the ZFT technique (Table 1), and 3 samples yielded suitable apatite grains for the AFT technique (Table 2), 2 of these 3 samples provided adequate horizontal confined track lengths (HCTLs) for the thermal history modelling.

**4.1 ZFT Technique:** The ZFT analyzed samples have successfully passed the statistical test of Chi-square ( $\chi^2$ ) which examine age homogeneity representing no evidence for several age populations (Table 2). Uranium concentrations in our zircons are of ca. 361 and 344  $\mu\text{g/g}$  (Table 1). The relationship between single grains ZFT ages and the corresponding  $^{238}\text{U}$  concentrations is entirely absent indicating that the metamictization effect can be neglected (Fig. 3).

Table 1 Zircon fission-track samples description, ages, and corresponding data.												
S.-Code	Elev. [m a.s.l.]	Coordinates Decimal		Lithology	$^{238}\text{U}$	n	$\rho_s$	$N_s$	$\chi^2$ [%]	Age [Ma]		
		N	E		[ $\mu\text{g/g}$ ]					W.M.	$1\sigma$	MSWD
WM-02	383	28.455222°	33.721169°	Diorite	387.1	17	72.1	4302	0.86	<b>338.6</b>	9.8	0.72
WM-07	445	28.62544°	32.44434°	Syenogranite	272.3	23	49.1	4725	0.92	<b>333.6</b>	8.7	0.68

Samples and zircon fission-track data represented as W.M.; weighted mean ages with 1-sigma ( $\sigma$ ) uncertainties. S.-Code; samples coode, Elev.; the elevation above sea-level of each sample in meters, U; concentration of  $^{238}\text{U}$  in  $\mu\text{g/g}$ , n; number of zircons where tracks were counted,  $\rho_s$ ; spontaneous tracks densities ( $10^6 \text{ tr/cm}^2$ ),  $N_s$ ; number of counted fission tracks,  $\chi^2$ ; chi square test values, MSWD; Mean Sum Weighted Deviates.

The resulting ZFT weighted mean thermochronological ages and the consistent  $1\sigma$  standard errors are  $339 \pm 10 \text{ Ma}$  and  $334 \pm 9 \text{ Ma}$  (Fig. 2), demonstrating cooling throw the PAZ of ZFT technique ( $240\text{--}200^\circ\text{C}$ ; [73]) since ca.  $337 \pm 10 \text{ Ma}$ . These ages are accordant with the published ZFT ages on different regions of the northern ANS, which were interpreted as a Devonian-Carboniferous tectonic caused exhumation [25], [59], [74]–[76]. This uplift is also consistent with the regional stratigraphic sequence suggesting a previous existence of more than 2.5 km of a Lower Palaeozoic sequence.

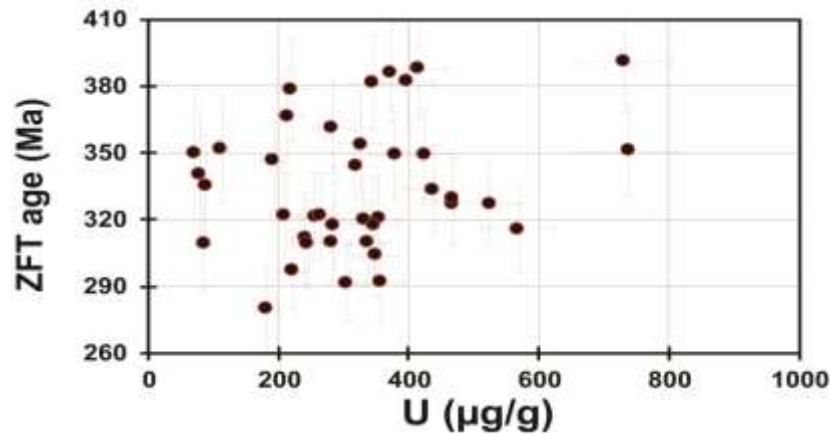


**Fig. (3):** A ZFT ages against  $^{238}\text{U}$  concentrations plot, representing an absence of any systematic pattern and any metamictization effect on the calculated ZFT ages.

**4.2 AFT Technique:** The AFT analyzed samples provided cooling ages in the range between  $26 \pm 5$  Ma and  $21 \pm 4$  Ma (Table 2), documenting for cooling throw the PAZ of the AFT technique ( $110\text{--}60$  °C; [77], [78]) at ca.  $24 \pm 5$  Ma (Fig. 2; Table 2). Similar cooling ages are reported from other localities of the ANS [24], [26], [30], [33].

The obtained AFT cooling ages have reset during the rift-related exhumation event indicating an uplift across the PAZ of the AFT technique. In other words, the rift flanks in the area of study exhumed the rift flanks from temperatures greater than the AFT closure temperature ( $110$  °C).

**Table 2** Apatite fission-track age details, sample descriptions, and track length data.

S.-No.	Elev. [m a.s.l.]	Coordinates Decimal		Lithology	<sup>238</sup> U	n	$\rho_{\sigma}$	$N_s$	$\chi^2$ [%]	W.M. Age	1 $\sigma$	Lc	SD	Dpar	SD
		N	E		[ $\mu$ g/g]		(X10 <sup>6</sup> track/cm <sup>2</sup> )			[Ma]		(μm)		(μm)	
Group A															
WM-01	320	28.443919°	33.698517°	Diorite	NA	NA	NA	NA	NA	NA	NA	NA	NA	NA	NA
WM-02	383	28.455222°	33.721169°	Syenite	9.5	22	0.1	46	0.94	20.5	3.7	13.4	1.3	1.6	0.2
WM-03	409	28.460097°	33.746803°	Syenite	NA	NA	NA	NA	NA	NA	NA	NA	NA	NA	NA
WM-04	445	28.464642°	33.756833°	Syenite	11.1	20	0.1	51	0.89	23.0	3.9	12.5	1.5	1.6	0.1
WM-05	482	28.472203°	33.762306°	Diorite	NA	NA	NA	NA	NA	NA	NA	NA	NA	NA	NA
WM-06	325	28.501806°	33.678408°	Diorite	NA	NA	NA	NA	NA	NA	NA	NA	NA	NA	NA
WM-07	445	28.533856°	33.695886°	Syenite	7.4	20	0.1	45	0.92	25.9	4.6	13.3	1.7	1.4	0.2

Sample information and apatite fission-track data are given as weighted mean ages with 1-sigma ( $\sigma$ ) uncertainties. Lc; mean track length after c-axis correction, Dpar; mean etch pit diameter. More details are provided in Table 1.

**4.3 Thermal History Modelling:** The time-temperature (t-T) history was reconstructed by HeFTy v1.9 code [70]. The Monte Carlo algorithm in HeFTy is guided by user-defined t-T constraints. We have defined these constraints from the calculated ZFT and AFT cooling ages and the reported geologic events; the Precambrian post-assembly event of erosion (PAEE), when the whole ENS was destructed, and the Red Sea/Suez Rift during the Oligocene-Miocene (Fig. 4). The extend of these constraints on the time axis was fixed according to the obtained ages and level of uncertainties of each tectonic activity.

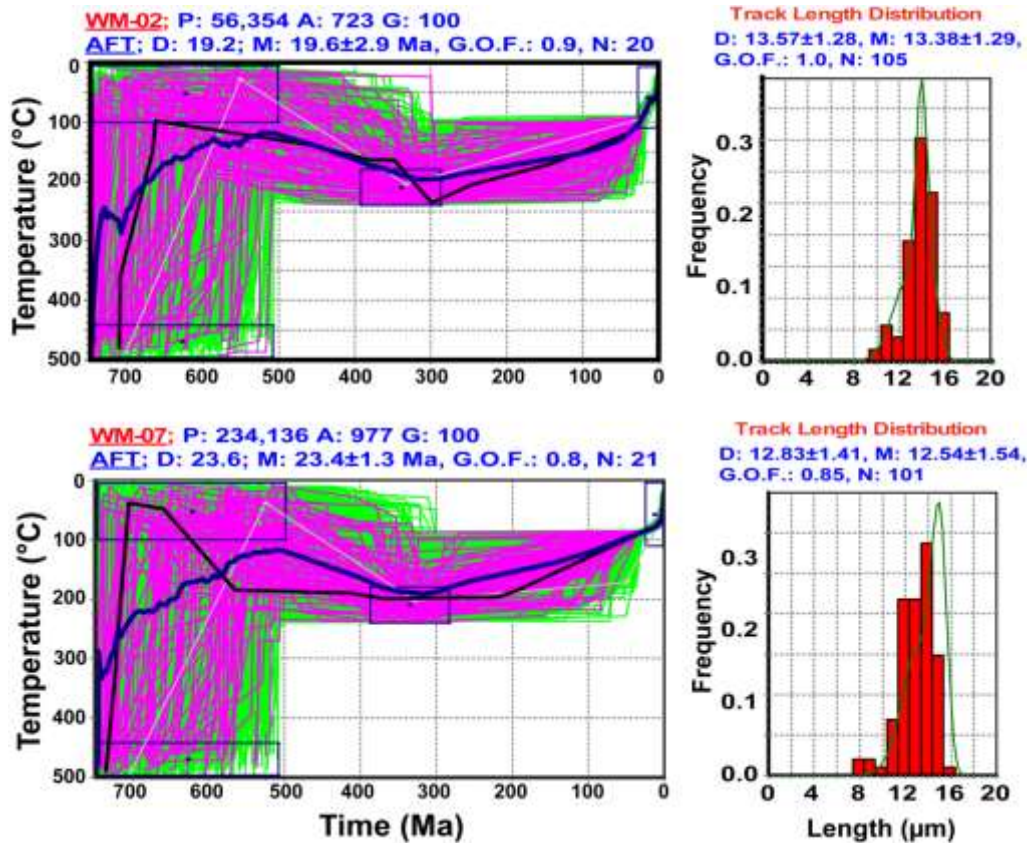


**Fig. (4):** Thermal history models reconstructed using the HeFTy code [72]. The resulting t–T paths represent four levels of reliability; acceptable fit (green), good fit (purple), the best fit (black), and the weighted mean (blue) paths [71], [72]. Four constraints were used to limit the modelling randomness, where the 1<sup>st</sup> represented the initial box at depth, the 2<sup>nd</sup> represents the post-accretion-related exhumation event, the 3<sup>rd</sup> shows the ZFT age, and the 4<sup>th</sup> shows the AFT age. Where, WM-02: sample code, P: number of inverse iterations, A: acceptable fit models' number, G: good fit models' number, D: calculated AFT ages and CLs (1- $\sigma$  error), M: model calculated AFT ages and CLs, G.O.F.: goodness of fit, N: number of single grains and CLs.

The t-T models recommend a first quick exhumation activity through the Neoproterozoic to uplift samples near the surface of the earth. This uplifting event is caused by the PAEE, which completely eroded the ENS basement before Cambrian time, however, the position of the recent rock exposures during the Cambrian is unknown as they might have been exposed to the surface or buried in the subsurface. Unfortunately, the t-T models could not provide exclusive answers. Afterwards, the study area experienced burial/reheating event beneath the Lower Palaeozoic sequence till Carboniferous time (Fig. 4). Then, a Devonian-Carboniferous rapid cooling event occurred causing uplifting to the PAZ of the AFT technique as an effect of the Hercynian activity, causing the removal of ca. 2.5 km of the sedimentary sequence and the basement rocks (e.g., [58]). This uplift is marked sedimentologically by changing the depositional regime from the Um Bogma marine Formation (Lower Carboniferous) to the erosional Abu Darag Formation (Upper Carboniferous) [79], [80]. Then, the region experienced a rapid exhumation event during the Oligocene-Miocene (Fig. 4), as a response to the northern Red Sea/Suez Rift system. These AFT ages (Fig. 2; Table 2) indicate exhumation from depths greater than 110 °C equivalent temperatures (Fig. 4).

## 5- INTERPRETATION

The produced cooling ages and the reconstructed thermal/tectonic histories document three rock uplifting activities that occurred as a response to four events; (1) the Neoproterozoic PAEE, which caused a consequential rocks exhumation through the isostatic rebound. Then, the basement rocks were reburied beneath a Lower Paleozoic sequence of more than 2.5 km. (2) the Devonian-Carboniferous tectonic activity, which resulted in rock exhumations and removal of the Lower Palaeozoic sequence and portions

of the basement. (3) the Oligo-Miocene opening of the Suez Rift, which resulted in rift flanks exhumation from depths greater than 110 °C equivalent temperatures.

## 6- CONCLUSION

Three events have affected and reshaped the studied eastern flank of the Suez rift;

- The PAEE uplifted rocks from emplacement depths to near the surface.
- The Hercynian tectonic activity has affected the studied region through rock exhumations.
- The Rift opening was accompanied by rift flanks exhumation from depths greater than 110 °C equivalent temperatures.

## 7- REFERENCES

- [1] T. M. Kusky, M. Abdelsalam, R. D. Tucker, and R. J. Stern, "Evolution of the East African and related orogens, and the assembly of Gondwana," *Precambrian Research*, vol. 123, no. 2, pp. 81–85, Jun. 2003, doi: 10.1016/S0301-9268(03)00062-7.
- [2] J. G. Meert, "A synopsis of events related to the assembly of eastern Gondwana," *Tectonophysics*, vol. 362, no. 1–4, pp. 1–40, Feb. 2003, doi: 10.1016/S0040-1951(02)00629-7.
- [3] R. J. Stern, "ARC Assembly and Continental Collision in the Neoproterozoic East African Orogen: Implications for the Consolidation of Gondwanaland," *Annu. Rev. Earth Planet. Sci.*, vol. 22, no. 1, pp. 319–351, May 1994, doi: 10.1146/annurev.earth.22.050194.001535.
- [4] S. Mansour, N. Hasebe, J. G. Meert, A. Tamura, F. I. Khalaf, and M. K. El-Shafei, "Evolution of the Arabian-Nubian Shield in Gabal Samra area, Sinai; implications from zircon U–Pb geochronology," *Journal of African Earth Sciences*, vol. 192, p. 104538, Aug. 2022, doi: 10.1016/j.jafrearsci.2022.104538.
- [5] B. H. Ali, S. A. Wilde, and M. M. A. Gabr, "Granitoid evolution in Sinai, Egypt, based on precise SHRIMP U–Pb zircon geochronology," *Gondwana Research*, vol. 15, no. 1, pp. 38–48, Feb. 2009, doi: 10.1016/j.gr.2008.06.009.
- [6] M. Z. El-Bialy, "On the Pan-African transition of the Arabian–Nubian Shield from compression to extension: The post-collision Dokhan volcanic suite of Kid-Malhak region, Sinai, Egypt," *Gondwana Research*, vol. 17, no. 1, pp. 26–43, Jan. 2010, doi: 10.1016/j.gr.2009.06.004.
- [7] H. A. Eliwa, J.-I. Kimura, and T. Itaya, "Late Neoproterozoic Dokhan Volcanics, North Eastern Desert, Egypt: Geochemistry and petrogenesis," *Precambrian Research*, vol. 151, no. 1, pp. 31–52, Dec. 2006, doi: 10.1016/j.precamres.2006.08.005.
- [8] H. A. Eliwa, M. Z. El-Bialy, and M. Murata, "Ediacaran post-collisional volcanism in the Arabian-Nubian Shield: The high-K calc-alkaline Dokhan Volcanics of Gabal Samr El-Qaa (592±5Ma), North Eastern Desert, Egypt," *Precambrian Research*, vol. 246, pp. 180–207, Jun. 2014, doi: 10.1016/j.precamres.2014.03.015.
- [9] M. Eyal, B. Litvinovsky, B. M. Jahn, A. Zandvilevich, and Y. Katzir, "Origin and evolution of post-collisional magmatism: Coeval Neoproterozoic calc-alkaline and alkaline suites of the Sinai Peninsula," *Chemical Geology*, vol. 269, no. 3, pp. 153–179, Jan. 2010, doi: 10.1016/j.chemgeo.2009.09.010.
- [10] P. R. Johnson *et al.*, "Late Cryogenian–Ediacaran history of the Arabian–Nubian Shield: A review of depositional, plutonic, structural, and tectonic events in the closing stages of the northern East African Orogen," *Journal of African Earth Sciences*, vol. 61, no. 3, pp. 167–232, Oct. 2011, doi: 10.1016/j.jafrearsci.2011.07.003.
- [11] S. Mansour, N. Hasebe, E. Azab, A. Y. Elnaggar, and A. Tamura, "Combined Zircon/Apatite U-Pb and Fission-Track Dating by LA-ICP-MS and Its Geological

- Applications: An Example from the Egyptian Younger Granites,” *Minerals*, vol. 11, no. 12, Art. no. 12, Dec. 2021, doi: 10.3390/min11121341.
- [12] A. M. Moghazi, “Geochemistry and petrogenesis of a high-K calc-alkaline Dokhan Volcanic suite, South Safaga area, Egypt: the role of late Neoproterozoic crustal extension,” *Precambrian Research*, vol. 125, no. 1, pp. 161–178, Jul. 2003, doi: 10.1016/S0301-9268(03)00110-4.
- [13] R. Ressetar and J. R. Monrad, “Chemical composition and tectonic setting of the Dokhan Volcanic Formation, Eastern Desert, Egypt,” *Journal of African Earth Sciences* (1983), vol. 1, no. 2, pp. 103–112, Jan. 1983, doi: 10.1016/0899-5362(83)90002-7.
- [14] C. Breitkreuz *et al.*, “Neoproterozoic SHRIMP U–Pb zircon ages of silica-rich Dokhan Volcanics in the North Eastern Desert, Egypt,” *Precambrian Research*, vol. 182, no. 3, pp. 163–174, Oct. 2010, doi: 10.1016/j.precamres.2010.06.019.
- [15] K. Kolodner, D. Avigad, M. McWILLIAMS, J. L. Wooden, T. Weissbrod, and S. Feinstein, “Provenance of north Gondwana Cambrian–Ordovician sandstone: U–Pb SHRIMP dating of detrital zircons from Israel and Jordan,” *Geol. Mag.*, vol. 143, no. 3, pp. 367–391, May 2006, doi: 10.1017/S0016756805001640.
- [16] B. P. Kohn, M. Eyal, and S. Feinstein, “A major Late Devonian–Early Carboniferous (Hercynian) Thermotectonic event at the NW Margin of the Arabian–Nubian Shield: Evidence from zircon fission track dating,” *Tectonics*, vol. 11, no. 5, pp. 1018–1027, Oct. 1992, doi: 10.1029/92TC00636.
- [17] G. M. Stampfli, J. F. von Raumer, and G. D. Borel, “Paleozoic evolution of pre-Variscan terranes: From Gondwana to the Variscan collision,” in *Variscan–Appalachian dynamics: The building of the late Paleozoic basement*, Boulder, USA: Geological Society of America, 2002. doi: 10.1130/0-8137-2364-7.263.
- [18] A. S. Alsharhan and A. E. M. Nairn, *Sedimentary Basins and Petroleum Geology of the Middle East*. Elsevier, 1997. doi: 10.1016/B978-0-444-82465-3.X5000-1.
- [19] M. Y. Meneisy, “Mesozoic igneous activity in Egypt,” *Qatar University Science Bulletin*, no. 6, 1986.
- [20] S. Sakran, A. A. Shehata, O. Osman, and M. El-Sherbiny, “Superposed tectonic regimes in west Beni Suef basin, Nile Valley, Egypt: Implications to source rock maturation and hydrocarbon entrapment,” *Journal of African Earth Sciences*, vol. 154, pp. 1–19, Jun. 2019, doi: 10.1016/j.jafrearsci.2019.03.010.
- [21] A. A. Shehata, F. M. El Fawal, M. Ito, M. A. Aboulmagd, and H. L. Brooks, “Senonian platform-to-slope evolution in the tectonically-influenced Syrian Arc sedimentary belt: Beni Suef Basin, Egypt - ScienceDirect,” *Journal of African Earth Sciences*, vol. 170, p. <https://doi.org/10.1016/j.jafrearsci.2020.103934>, 2020.
- [22] J. Barbarand, F. O. Marques, A. Hildenbrand, R. Pinna-Jamme, and C. R. Nogueira, “Thermal evolution of onshore West Iberia: A better understanding of the ages of breakup and rift-to-drift in the Iberia–Newfoundland Rift,” *Tectonophysics*, vol. 813, p. 228926, Aug. 2021, doi: 10.1016/j.tecto.2021.228926.
- [23] S. Mansour *et al.*, “New Insights into the thermo-tectonic evolution of the Arabian–Nubian Shield in Sinai, and the role of Mantle Plume in the Gulf of Suez Rifting,” *Tectonophysics*, 2022b.
- [24] N. Morag, I. Haviv, M. Eyal, B. P. Kohn, and S. Feinstein, “Early flank uplift along the Suez Rift: Implications for the role of mantle plumes and the onset of the Dead Sea Transform,” *Earth and Planetary Science Letters*, vol. 516, pp. 56–65, Jun. 2019, doi: 10.1016/j.epsl.2019.03.002.
- [25] A.-V. Bojar, H. Fritz, S. Kargl, and W. Unzog, “Phanerozoic tectonothermal history of the Arabian–Nubian shield in the Eastern Desert of Egypt: evidence from fission track and paleostress data,” *Journal of African Earth Sciences*, vol. 34, no. 3–4, pp. 191–202, Apr. 2002, doi: 10.1016/S0899-5362(02)00018-0.



- [26] S. Feinstein *et al.*, “Uplift and denudation history of the eastern Dead Sea rift flank, SW Jordan: Evidence from apatite fission track thermochronometry,” *Tectonics*, vol. 32, no. 5, pp. 1513–1528, 2013, doi: 10.1002/tect.20082.
- [27] B. P. Kohn, S. Feinstein, D. A. Foster, M. S. Steckler, and M. Eyal, “Thermal history of the eastern Gulf of Suez, II. Reconstruction from apatite fission track and K-feldspar measurements,” *Tectonophysics*, vol. 283, no. 1–4, pp. 219–239, Dec. 1997, doi: 10.1016/S0040-1951(97)00069-3.
- [28] B. P. Kohn and M. Eyal, “History of uplift of the crystalline basement of Sinai and its relation to opening of the Red Sea as revealed by fission track dating of apatites,” *Earth and Planetary Science Letters*, vol. 52, no. 1, pp. 129–141, Jan. 1981, doi: 10.1016/0012-821X(81)90215-6.
- [29] A. Kroner, W. Todt, I. Hussein, M. Mansour, and A. Rashwan, “Dating of late Proterozoic ophiolites in Egypt and the Sudan using the single grain zircon evaporation technique,” *Precambrian Research*, vol. 59, no. 1–2, pp. 15–32, Nov. 1992, doi: 10.1016/0301-9268(92)90049-T.
- [30] G. I. Omar, B. P. Kohn, T. M. Lutz, and H. Faul, “The cooling history of Silurian to Cretaceous alkaline ring complexes, south Eastern Desert, Egypt, as revealed by fission-track analysis,” *Earth and Planetary Science Letters*, vol. 83, no. 1–4, pp. 94–108, May 1987, doi: 10.1016/0012-821X(87)90054-9.
- [31] G. I. Omar and M. S. Steckler, “Fission Track Evidence on the Initial Rifting of the Red Sea: Two Pulses, No Propagation,” *Science*, vol. 270, no. 5240, pp. 1341–1344, Nov. 1995, doi: 10.1126/science.270.5240.1341.
- [32] M. S. Steckler, “Uplift and extension at the Gulf of Suez: indications of induced mantle convection,” *Nature*, vol. 317, no. 6033, pp. 135–139, Sep. 1985, doi: 10.1038/317135a0.
- [33] G. I. Omar, M. S. Steckler, W. R. Buck, and B. P. Kohn, “Fission-track analysis of basement apatites at the western margin of the Gulf of Suez rift, Egypt: evidence for synchronicity of uplift and subsidence,” *Earth and Planetary Science Letters*, vol. 94, no. 3–4, pp. 316–328, Sep. 1989, doi: 10.1016/0012-821X(89)90149-0.
- [34] S. Mansour, N. Hasebe, K. Abdelrahman, M. S. Fnaies, and A. Tamura, “Reconstructing the Tectonic History of the Arabian–Nubian Shield in Sinai: Low-Temperature Thermochronology Implications on Wadi Agar Area,” *Minerals*, vol. 13, no. 4, Art. no. 4, Apr. 2023, doi: 10.3390/min13040574.
- [35] S. Leroy *et al.*, “From rifting to oceanic spreading in the Gulf of Aden: a synthesis,” *Arab J Geosci*, vol. 5, no. 5, pp. 859–901, Sep. 2012, doi: 10.1007/s12517-011-0475-4.
- [36] R. Pik *et al.*, “Structural control of basement denudation during rifting revealed by low-temperature (U–Th–Sm)/He thermochronology of the Socotra Island basement—Southern Gulf of Aden margin,” *Tectonophysics*, vol. 607, pp. 17–31, Nov. 2013, doi: 10.1016/j.tecto.2013.07.038.
- [37] J. Serra-Kiel *et al.*, “Middle Eocene-Early Miocene larger foraminifera from Dhofar (Oman) and Socotra Island (Yemen),” *Arab J Geosci*, vol. 9, no. 5, p. 344, May 2016, doi: 10.1007/s12517-015-2243-3.
- [38] F. Watchorn, G. J. Nichols, and D. W. J. Bosence, “Rift-related sedimentation and stratigraphy, southern Yemen (Gulf of Aden),” in *Sedimentation and Tectonics in Rift Basins Red Sea:- Gulf of Aden*, B. H. Purser and D. W. J. Bosence, Eds., Dordrecht: Springer Netherlands, 1998, pp. 165–189. doi: 10.1007/978-94-011-4930-3\_11.
- [39] M. R. Hempton, “Structure and deformation history of the Bitlis suture near Lake Hazar, southeastern Turkey,” *Geol Soc America Bull*, vol. 96, no. 2, p. 233, 1985, doi: 10.1130/0016-7606(1985)96<233:SADHOT>2.0.CO;2.
- [40] C. J. Ebinger and N. H. Sleep, “Cenozoic magmatism throughout east Africa resulting from impact of a single plume,” *Nature*, vol. 395, no. 6704, pp. 788–791, Oct. 1998, doi: 10.1038/27417.

- [41] R. George, N. Rogers, and S. Kelley, "Earliest magmatism in Ethiopia: Evidence for two mantle plumes in one flood basalt province," *Geol*, vol. 26, no. 10, p. 923, 1998, doi: 10.1130/0091-7613(1998)026<0923:EMIEEF>2.3.CO;2.
- [42] T. O. Rooney, "The Cenozoic magmatism of East-Africa: Part I — Flood basalts and pulsed magmatism," *Lithos*, vol. 286–287, pp. 264–301, Aug. 2017, doi: 10.1016/j.lithos.2017.05.014.
- [43] W. Bosworth and D. F. Stockli, "Early magmatism in the greater Red Sea rift: timing and significance," *Can. J. Earth Sci.*, vol. 53, no. 11, pp. 1158–1176, Nov. 2016, doi: 10.1139/cjes-2016-0019.
- [44] C. Hofmann *et al.*, "Timing of the Ethiopian flood basalt event and implications for plume birth and global change," *Nature*, vol. 389, no. 6653, pp. 838–841, Oct. 1997, doi: 10.1038/39853.
- [45] A. ArRajehi *et al.*, "Geodetic constraints on present-day motion of the Arabian Plate: Implications for Red Sea and Gulf of Aden rifting," *Tectonics*, vol. 29, no. 3, p. 2009TC002482, Jun. 2010, doi: 10.1029/2009TC002482.
- [46] G. Cole *et al.*, "Petroleum geochemistry of the Midyan and Jaizan ba... ×," *Marine and Petroleum Geology*, vol. 12, pp. 597–614, Jan. 1995.
- [47] M. Stab, N. Bellahsen, R. Pik, X. Quidelleur, D. Ayalew, and S. Leroy, "Modes of rifting in magma-rich settings: Tectono-magmatic evolution of Central Afar: Modes of Rifting in Magma-Rich Settings," *Tectonics*, vol. 35, no. 1, pp. 2–38, Jan. 2016, doi: 10.1002/2015TC003893.
- [48] E. Szymanski, D. F. Stockli, P. R. Johnson, and C. Hager, "Thermochronometric evidence for diffuse extension and two-phase rifting within the Central Arabian Margin of the Red Sea Rift," *Tectonics*, vol. 35, no. 12, pp. 2863–2895, 2016, doi: 10.1002/2016TC004336.
- [49] S. C. Boone, M.-L. Balestrieri, and B. Kohn, "Thermo-tectonic imaging of the Gulf of Aden-Red Sea rift systems and Afro-Arabian hinterland," *Earth-Science Reviews*, vol. 222, p. 103824, Nov. 2021, doi: 10.1016/j.earscirev.2021.103824.
- [50] A. Kröner, J. Kröger, and A. A. A. Rashwan, "Age and tectonic setting of granitoid gneisses in the Eastern Desert of Egypt and south-west Sinai," *Geol Rundsch*, vol. 83, no. 3, pp. 502–513, Oct. 1994, doi: 10.1007/BF00194157.
- [51] R. J. Stern and C. E. Hedge, "Geochronologic and isotopic constraints on late Precambrian crustal evolution in the Eastern Desert of Egypt," *Am J Sci*, vol. 285, no. 2, Art. no. 2, Feb. 1985, doi: 10.2475/ajs.285.2.97.
- [52] J. P. Platt and P. C. England, "Convective removal of lithosphere beneath mountain belts; thermal and mechanical consequences," *American Journal of Science*, vol. 294, no. 3, pp. 307–336, Mar. 1994, doi: 10.2475/ajs.294.3.307.
- [53] R. Said, *The Geology of Egypt*, 2nd ed. Netherlands: A.A. Balkema, Rotterdam, 1990.
- [54] W. Bosworth, P. Huchon, and K. McClay, "The Red Sea and Gulf of Aden Basins," *Journal of African Earth Sciences*, vol. 43, no. 1–3, pp. 334–378, Oct. 2005, doi: 10.1016/j.jafrearsci.2005.07.020.
- [55] G. M. Stampfli, J. F. von Raumer, and G. D. Borel, "Paleozoic evolution of pre-Variscan terranes: From Gondwana to the Variscan collision," in *Variscan-Appalachian dynamics: The building of the late Paleozoic basement*, Boulder, USA: Geological Society of America, 2002. doi: 10.1130/0-8137-2364-7.263.
- [56] E. Klitzsch, "Plate tectonics and cratonal geology in Northeast Africa (Egypt, Sudan)," *Geologische Rundschau*, vol. 75, no. 3, pp. 755–768, Oct. 1986, doi: 10.1007/BF01820645.
- [57] E. Klitzsch, "Paleozoic," in *The Geology of Egypt*, R. Said, Ed., 2nd ed. Balkema, Rotterdam, 1990, pp. 451–486.
- [58] A. R. Moustafa and M. S. M. Yousif, "Structural evolution of the eastern shoulder of the Suez Rift: Um Bogma area," *Neues Jahrbuch für Geologie und Paläontologie* -

- Monatshefte*, vol. 1993, no. 11, pp. 655–668, Nov. 1993, doi: 10.1127/njgpm/1993/1993/655.
- [59] B. P. Kohn, M. Eyal, and S. Feinstein, “A major Late Devonian-Early Carboniferous (Hercynian) Thermotectonic event at the NW Margin of the Arabian-Nubian Shield: Evidence from zircon fission track dating,” *Tectonics*, vol. 11, no. 5, pp. 1018–1027, Oct. 1992, doi: 10.1029/92TC00636.
- [60] J. F. Dewey, W. C. Pitman, W. B. F. Ryan, and J. Bonnin, “Plate Tectonics and the Evolution of the Alpine System,” *Geological Society of America Bulletin*, vol. 84, no. 10, p. 3137, 1973, doi: 10.1130/0016-7606(1973)84<3137:PTATEO>2.0.CO;2.
- [61] R. W. Girdler, “Problems concerning the evolution of oceanic lithosphere in the northern Red Sea,” *Tectonophysics*, vol. 116, no. 1, pp. 109–122, Jun. 1985, doi: 10.1016/0040-1951(85)90224-0.
- [62] S. Feinstein, B. P. Kohn, M. S. Steckler, and M. Eyal, “Thermal history of the eastern margin of the Gulf of Suez, I. reconstruction from borehole temperature and organic maturity measurements,” *Tectonophysics*, vol. 266, no. 1–4, pp. 203–220, Dec. 1996, doi: 10.1016/S0040-1951(96)00190-4.
- [63] W. Bosworth, D. F. Stockli, and D. E. Helgeson, “Integrated outcrop, 3D seismic, and geochronologic interpretation of Red Sea dike-related deformation in the Western Desert, Egypt – The role of the 23Ma Cairo ‘mini-plume,’” *Journal of African Earth Sciences*, vol. 109, pp. 107–119, Sep. 2015, doi: 10.1016/j.jafrearsci.2015.05.005.
- [64] G. A. Wagner, “Spaltspurenalter von Mineralen und natürlichen Gläsern: eine Übersicht.,” *Fortschritte der Mineralogie*, no. 49, pp. 114–145, 1972.
- [65] A. J. W. Gleadow and I. R. Duddy, “A natural long-term track annealing experiment for apatite,” *Nuclear Tracks*, vol. 5, no. 1–2, pp. 169–174, Jun. 1981, doi: 10.1016/0191-278X(81)90039-1.
- [66] R. Yamada, T. Tagami, S. Nishimura, and H. Ito, “Annealing kinetics of fission tracks in zircon: an experimental study,” *Chemical Geology*, vol. 122, no. 1–4, pp. 249–258, May 1995, doi: 10.1016/0009-2541(95)00006-8.
- [67] J. I. Garver, “Etching zircon age standards for fission-track analysis,” *Radiation Measurements*, vol. 37, no. 1, pp. 47–53, Feb. 2003, doi: 10.1016/S1350-4487(02)00127-0.
- [68] A. J. W. Gleadow, I. R. Duddy, and J. F. Lovering, “Fission track analysis: A new tool for the evaluation of thermal histories and hydrocarbon potential,” *The APPEA Journal*, vol. 23, no. 1, Art. no. 1, 1983, doi: 10.1071/AJ82009.
- [69] P. Vermeesch, “IsoplotR: A free and open toolbox for geochronology,” *Geoscience Frontiers*, vol. 9, no. 5, pp. 1479–1493, Sep. 2018, doi: 10.1016/j.gsf.2018.04.001.
- [70] R. A. Ketcham, “Forward and Inverse Modeling of Low-Temperature Thermochronometry Data,” *Reviews in Mineralogy and Geochemistry*, vol. 58, no. 1, pp. 275–314, Jan. 2005, doi: 10.2138/rmg.2005.58.11.
- [71] R. A. Ketcham, “HeFTy version 1.6.7, Manual.” 2009.
- [72] R. A. Ketcham, R. A. Donelick, M. L. Balestrieri, and M. Zattin, “Reproducibility of apatite fission-track length data and thermal history reconstruction,” *Earth and Planetary Science Letters*, vol. 284, no. 3, pp. 504–515, Jul. 2009, doi: 10.1016/j.epsl.2009.05.015.
- [73] M. Bernet, M. Brandon, J. Garver, M. L. Balestrieri, B. Ventura, and M. Zattin, “Exhuming the Alps through time: clues from detrital zircon fission-track thermochronology,” *Basin Research*, vol. 21, no. 6, pp. 781–798, 2009, doi: 10.1111/j.1365-2117.2009.00400.x.
- [74] B. Kohn, T. Weissbrod, L. Chung, K. Farley, and S. Bodorkos, “Low-temperature thermochronology of francolite: Insights into timing of Dead Sea Transform motion,” *Terra Nova*, vol. 31, no. 3, pp. 205–219, Jun. 2019, doi: 10.1111/ter.12387.
- [75] P. Vermeesch, D. Avigad, and M. O. McWilliams, “500 m.y. of thermal history elucidated by multi-method detrital thermochronology of North Gondwana Cambrian sandstone (Eilat

- area, Israel),” *GSA Bulletin*, vol. 121, no. 7–8, pp. 1204–1216, Jul. 2009, doi: 10.1130/B26473.1.
- [76] S. Mansour, M. A. Gharib, N. Hasebe, K. Abdelrahman, M. S. Fnais, and A. Tamura, “Tectonic evolution of the Gabal Loman area, North Eastern Desert, Egypt: implications from low-temperature multithermochronometry on the Arabian-Nubian shield,” *Front. Earth Sci.*, vol. 11, no. 1193692, p. 15, Jul. 2023, doi: 10.3389/feart.2023.1193692.
- [77] R. A. Donelick, P. B. O’Sullivan, and R. A. Ketcham, “3. Apatite Fission-Track Analysis,” in *Low-Temperature Thermochronology*, P. W. Reiners and T. A. Ehlers, Eds., Berlin, Boston: De Gruyter, 2005, pp. 49–94. doi: 10.1515/9781501509575-005.
- [78] A. J. W. Gleadow, I. R. Duddy, P. F. Green, and J. F. Lovering, “Confined fission track lengths in apatite: a diagnostic tool for thermal history analysis,” *Contributions to Mineralogy and Petrology*, vol. 94, no. 4, pp. 405–415, Dec. 1986, doi: 10.1007/BF00376334.
- [79] M. Darwish and A. El Araby, “Petrography and diagenetic aspects of some siliclastic hydrocarbon reservoirs in relation to rifting of the Gulf of Suez, Egypt. Geodynamics and sedimentation of the Red Sea—Gulf of Aden Rift system,” *Egyptian J. Geol.*, vol. 3, pp. 1–25, 1994.
- [80] N. Tewfik, C. Harwood, and I. Deighton, “The Miocene, Rudeis and Kareem Formations in the Gulf of Suez: Aspects of sedimentology and geochemistry,” *EGPC Exploration Seminar, Cairo, i*, vol. 11, pp. 84–113, 1992.